Biochemistry **1998,** *37,* 10469−10477

Oxidase Activity of the Acyl-CoA Dehydrogenases[†]

Edith R. DuPlessis,[‡] Jackson Pellett,[§] Marian T. Stankovich,[§] and Colin Thorpe*[,‡]

Department of Chemistry and Biochemistry, University of Delaware, Newark, Delaware 19716, and Department of Chemistry, 207 Pleasant St. S.E., University of Minnesota, Minneapolis, Minnesota 55455

Received April 6, 1998; Revised Manuscript Received May 14, 1998

ABSTRACT: The medium chain acyl-CoA dehydrogenase catalyzes the flavin-dependent oxidation of a variety of acyl-CoA thioesters with the transfer of reducing equivalents to electron-transferring flavoprotein. The binding of normal substrates profoundly suppresses the reactivity of the reduced enzyme toward molecular oxygen, whereas the oxidase reaction becomes significant using thioesters such as indolepropionyl-CoA (IP-CoA) and 4-(dimethylamino)-3-phenylpropionyl-CoA (DP-CoA). Steady-state and stopped-flow studies with IP-CoA led to a kinetic model of the oxidase reaction in which only the free reduced enzyme reacts with oxygen (Johnson, J. K., Kumar, N. R., and Srivastava, D. K. (1994) *Biochemistry 33*, 4738−4744). We have tested their proposal with IP-CoA and DP-CoA. The dependence of the oxidase reaction on oxygen concentration is biphasic with a major low affinity phase incompatible with a model predicting a simple K_m for oxygen of 3 μM. If only free reduced enzyme reacts with oxygen, increasing IP-CoA would show strong substrate inhibition because it binds tightly to the reduced enzyme. Experimentally, IP-CoA shows simple saturation kinetics. The Glu376-Gln mutant of the medium chain dehydrogenase allows the oxygen reactivity of complexes of the reduced enzyme with IP-CoA and the corresponding product indoleacryloyl-CoA (IA-CoA) to be characterized without the subsequent redox equilibration that complicates analysis of the oxidase kinetics of the native enzyme. In sum, these data suggest that when bulky, nonphysiological substrates are employed, multiple reduced enzyme species react with molecular oxygen. The relatively high oxidase activity of the short chain acyl-CoA dehydrogenase from the obligate anaerobe *Megasphaera elsdenii* was studied by rapid reaction kinetics of wild-type and the Glu367-Gln mutant using butyryl-, crotonyl-, and 2-aza-butyryl-CoA thioesters. In marked contrast to those of the mammalian dehydrogenase, complexes of the reduced bacterial enzyme with these ligands react with molecular oxygen at rates similar to those of the free protein. Evolutionary and mechanistic aspects of the suppression of oxygen reactivity in the acyl-CoA dehydrogenases are discussed.

The factors which modulate the oxygen reactivity of flavoproteins are still poorly understood (*1*). This paper reexamines the behavior of two representative classes of the acyl-CoA dehydrogenase family (*2*−*6*) toward molecular oxygen. The early studies of Beinert and colleagues defined key elements of both the reductive and oxidative halves of normal catalysis in these dehydrogenases (*2*, *7*, *8*). Reduction of the medium chain dehydrogenase occurs rapidly with an optimal substrate such as octanoyl-CoA (*2*, *9*, *10*) generating an unusually air-stable charge-transfer complex between the reduced enzyme and a very tightly bound molecule of the product, *trans*-2-octenoyl-CoA (*2*, *8*, *11*−*13*). Thereafter, two sequential 1-electron transfers to two molecules of the electron-transferring flavoprotein yields the oxidized dehydrogenase•enoyl-CoA complex (*14*−*17*). Subsequent dissociation of the product completes catalysis. Several possible reasons for this ternary complex mechanism have been discussed (*6*, *13*, *17*). First, the extremely tight binding of octenoyl-CoA to the reduced enzyme ensures that the octanoyl-CoA can effectively reduce the oxidized medium chain dehydrogenase. Electrochemical studies show that, in the absence of this strong preferential binding of the product, the substrate would not significantly reduce the dehydrogenase (*18*). Second, the bound product greatly accelerates the interflavin electron transfer to ETF at both dihydroflavin and semiquinone levels (*15*, *17*). Finally, enoyl-CoA binding to the reduced enzyme profoundly suppresses its reaction with molecular oxygen (*2*, *3*, *6*, *12*), thereby avoiding a wasteful and damaging accumulation of reduced oxygen species in the mammalian mitochondrial matrix.

A series of redox inactive acyl-CoA analogues was tested to explore those structural aspects of enoyl-CoA product which were necessary for the profound suppression of the oxidase reaction of the pig kidney dehydrogenase (*12*). In each case, the rate of reoxidation of the dihydroflavin form of the enzyme was followed in the presence of saturating concentrations of ligand in the stopped-flow spectrophotometer. These complexes showed a range of reactivity: some conferred essentially no protection, while others suppressed the reactivity of the free enzyme 3000-fold (*12*). The single most important factor in lowering oxygen reactivity was the presence of the thioester carbonyl group. Increasing the chain length exerts a much more modest effect. These data,

---

[†] This work was supported in part by NIH Grants GM26643 (C.T.) and GM29344 (M.S.).

* To whom correspondence should be addressed.

[‡] University of Delaware.

[§] University of Minnesota.

S0006-2960(98)00767-3 CCC: $15.00

together with that provided by the reoxidation of flavins in model systems (*19*), suggested that the variable suppression of oxygen reactivity might depend on the degree of ligand-induced desolvation of the active site of the medium chain dehydrogenase (*6*, *12*).

A different view of the oxidase activity of the dehydrogenase has been suggested in a series of papers by Srivastava and colleagues (*20*−*28*). They synthesized a chromophoric substrate, IP-CoA[1] (*20*, *29*), and studied its interaction with the dehydrogenase by steady state and rapid reaction approaches (*20*−*23*). They concluded that oxygen accepts electrons from the free reduced enzyme only (*23*−*26*). These data obtained with the chromophoric substrate IP-CoA seem at variance with the results described above for less bulky, straight-chained, acyl-CoA analogues (*14*, *28*). We have therefore reexamined the kinetic scheme proposed by Srivastava and colleagues to explain the oxidase activity of the acyl-CoA dehydrogenase toward IP-CoA under the conditions used previously. Two critical predictions of this model are not met. We have extended our studies using a second chromophoric substrate of the medium chain enzyme and have also tested another representative of the acyl-CoA dehydrogenase family. In sum, the present results show that oxygen interacts not just with the free enzyme but also with several reduced enzyme species. These new data underscore the complexity of such an apparently simple reaction as the reoxidation of the acyl-CoA dehydrogenase by molecular oxygen.

MATERIALS AND METHODS

Materials. CoASH (lithium salt), butyryl-CoA, crotonoyl-CoA, octanoyl-CoA, and glucose oxidase were from Sigma. Ferrocenium hexafluorophosphate, 3-indolepropionic, *trans*-3-indoleacrylic, and 4-dimethylaminocinnamic acids were obtained from Aldrich. Sodium dithionite was obtained from the Virginia Smelting Co., Portsmouth, VA. 5-Deazariboflavin was a generous gift from Drs. Sandro Ghisla and Vincent Massey. IP-CoA, IA-CoA, DP-CoA, and DC-CoA thioesters were prepared using the corresponding acids via the mixed anhydride procedure of Bernert and Sprecher (*30*). 4-Dimethylamino-3-phenylpropionic acid was made by reducing the acrylic acid by the procedure of Boudjouk and Han (*25*, *31*), and its structure was verified via ^{1}H NMR. 2-Azaoctanoyl- and 2-azabutyryl-CoA were prepared as described previously (*12*). Thioesters were purified on semipreparative octadecylsilica HPLC columns as described by Cummings and Thorpe (*32*). Purified thioesters were desalted using gel filtration on Bio-Gel P-2 (Bio-Rad Laboratories). Thioester concentrations were determined via UV/visible spectroscopy with a Hewlett-Packard 8452A diode array spectrophotometer, using the following molar extinction coefficients (*25*): IP-CoA, 18.2 mM^{-1} cm^{-1} at 260 nm; IA-CoA, 26.5 mM^{-1} cm^{-1} at 368 nm; DP-CoA, 19.4 mM^{-1} cm^{-1} at 250 nm; and DC-CoA, 20.6 mM^{-1} cm^{-1} at 400 nm.

Human MCAD Expression in Escherichia coli. *E. coli* BL21 (DE3) cells (Novagen) transformed with the recombinant human medium chain acyl-CoA dehydrogenase/pET11a clone were a generous gift of Dr. A. W. Strauss (Washington University, St. Louis, MO). The pTrc/E376Q mutant expressed in TG1 *E. coli* cells was a kind gift of Dr. Sandro Ghisla (University of Konstanz, Konstanz, Germany). Cells were grown in a rich culture medium (*33*), pH 7.1, containing 100 μg/mL ampicillin in culture flasks at 25 °C for 24 h. Induction was not necessary since basal levels of expression due to the leakiness of the *lacUV5* promotor were sufficient for purification of 18 mg of MCAD per liter of culture.

Enzymes. Medium chain acyl-CoA dehydrogenase was isolated from pig kidney as described previously (*11*, *15*, *34*) with some modifications. The calcium phosphate chromatography step was omitted. Following chromatography on octyl Sepharose CL 4B, an FPLC Source 15PHE HR10/10 column (Pharmacia Biotech) was employed as a final purification step. The enzyme was obtained with a 280/446 nm absorbance ratio of 5.2 or less. A molar extinction coefficient of 15.4 mM^{-1} cm^{-1} at 446 nm (*11*) was used to determine enzyme concentration.

Purification of the recombinant human wild-type MCAD and the corresponding Glu376-Gln mutant was based upon the pig kidney procedure (*11*, *15*, *34*) as described below. Frozen cells were thawed and resuspended in two volumes (w/v) of standard buffer (50 mM potassium phosphate, 0.3 mM EDTA), pH 7.2, containing 50 μM FAD. The cells were lysed by French Press, and cell debris was removed by centrifugation for 30 min at 10000*g*. MCAD was precipitated with 80% ammonium sulfate. The resulting pellet was resuspended in 20 mM potassium phosphate, 0.3 mM EDTA buffer, pH 7.2, and dialyzed against the same buffer containing 5 μM FAD. This sample was loaded onto a Q-Sepharose column (5 × 12 cm) equilibrated with the same buffer devoid of FAD. A linear gradient against 400 mM potassium phosphate, 0.3 mM EDTA, pH 7.2, was applied to the column. MCAD fractions were screened by UV/visible spectroscopy on a Hewlett-Packard HP8452A diode array spectrophotometer, pooled, concentrated, and washed in Centriprep-30 concentrators (Amicon, Corp.). The resulting enzyme sample was applied to a Source 15Q FPLC column (HR10/10, Pharmacia Biotech) in 20 mM phosphate buffer, pH 7.2. A linear gradient to 0.6 M potassium chloride, pH 7.2, was established via a Pharmacia FPLC P-500 pump system with a subsequent linear gradient to 1.2 M KCl. Fractions were monitored with a Pharmacia UV-M detector at 280 nm. Pooled fractions were precipitated with 80% ammonium sulfate. The pellet was redissolved in 20 mM potassium phosphate, 40% ammonium sulfate, pH 7.6, and applied to an FPLC Source 15PHE HR10/10 FPLC column (Pharmacia Biotech) equilibrated with the above buffer. The column was developed with a reverse linear gradient to 20 mM potassium phosphate, pH 7.6. MCAD fractions were pooled, concentrated, and washed in Centriprep-30 concentrators yielding enzyme with a 280/446 nm absorbance ratio of 5.2 or less. A molar extinction coefficient of 14.8 mM^{-1} cm^{-1} at 446 nm (*35*) was used to quantitate the human recombinant proteins.

Recombinant *Megasphaera elsdenii* SCAD and the Glu367-Gln mutant were purified as described previously (*36*) with minor modifications in the cell lysis procedure. The cell paste was resuspended in 1 volume (w/v) of 0.1 M phosphate

---

[1] Abbreviations: IP-CoA, indolepropionyl-CoA; IA-CoA, indoleacryloyl-CoA; DP-CoA, 4-(dimethylamino)-3-phenylpropionyl-CoA; DC-CoA, 4-dimethylaminocinnamoyl-CoA; MCAD, medium chain acyl-CoA dehydrogenase; SCAD, bacterial short chain acyl-CoA dehydrogenase; E_{ox}, oxidized MCAD; E_{red}, reduced MCAD.

buffer, pH 7.0, containing 100 μM FAD and 1 mg/mL lysozyme, and the mixture was stirred at room temperature for 15 min. The cells were disrupted by sonication in an ice−salt bath maintaining the temperature below 10 °C. Cell debris was removed by centrifugation for 30 min at 17600*g* and the crude extract used for further purification (*36*). Extinction coefficients for wild-type and mutant short chain enzymes were 14.2 mM^{-1} cm^{-1} at 450 nm (*36, 37*) and 13.9 mM^{-1} cm^{-1} at 452 nm (*36*), respectively.

General Methods. Unless stated otherwise, the standard buffer for MCAD was 50 mM potassium phosphate, pH 7.6, containing 0.3 mM EDTA. Experiments involving SCAD used the same buffer at pH 7.0. All experiments were performed at 25 °C. UV/visible measurements were obtained using either a Hewlett-Packard 8452A or a Perkin-Elmer 552A spectrophotometer. The standard ferrocenium (*38*) and DCIP/PMS (*39*) assays were used for MCAD and SCAD activity measurements, respectively. The oxidase activity of MCAD and SCAD followed product formation with substrates in standard buffer containing differing amounts of dissolved oxygen. Kinetic and binding parameters were analyzed using either Inplot (GraphPad) or Enzfitter (Elsevier Biosoft).

Anaerobic Procedures. Solutions were deoxygenated by repeated cycles of nitrogen and vacuum as described previously (*15*). Enzyme was reduced by titration with sodium dithionite or via photoreduction with 1 μM 5-deazariboflavin in standard buffer containing 5 mM EDTA (*40*).

Stopped-Flow Spectrophotometry. A Kinetics Instruments stopped-flow instrument equipped with a 2-cm path length cell was prepared for anaerobiosis as described previously (*41*). Data acquisition and analysis software was from On-Line Instuments Systems, Inc. Standard buffers were bubbled for 2 h at 25 °C with nitrogen, air, or oxygen as needed. Intermediate oxygen concentrations were prepared immediately before use by mixing volumes of these solutions containing the appropriate ligand concentrations, taking care to avoid gas bubbles and exposure to the atmosphere. Sodium dithionite or photoreduced enzyme was prepared anaerobically in tonometers and loaded onto the stopped-flow as before (*41*). All concentrations are quoted after mixing.

Reoxidation experiments with liganded reduced MCAD were carried out by first chemically reducing the enzyme in an anaerobic cuvette with a slight (1.05-fold) excess of sodium dithionite. Reduction was monitored with a Hewlett-Packard 8452A diode array spectrophotometer. Acyl-CoA ligands were then added anaerobically, followed by opening the cuvette to air and immediately adding sufficient oxygen-saturated standard buffer to yield a dissolved oxygen concentration of 240 μM. Reoxidation was monitored spectrophotometrically.

Computer Simulations. Simulations of Schemes 1−3 used an iterative routine written in QuickBASIC, incorporating the rate constants listed in Table 1. Typically, the enzyme concentration was set at 0.1 μM with an iteration time of 0.1 ms. The program evaluates the concentration of each species with time and was checked by mass balance and, where appropriate, by calculation of equilibrium constants predicted from the simulation compared to those implied by Table 1. Initial rates from this simulation were replotted and fit by nonlinear least squares using Inplot or Enzfitter.

Table 1: Rate Constants[a] Used in Simulation of Schemes 1−3

k_1	10^8 M^{-1} s^{-1}	k_4	1490 s^{-1}
k_{-1}	1150 s^{-1}	k_{-4}	10^8 M^{-1} s^{-1}
k_2	0.55 s^{-1}	k_5	2650 M^{-1} s^{-1}
k_{-2}	0.08 s^{-1}	k_6	10^8 M^{-1} s^{-1}
k_3	0.01 s^{-1}	k_{-6}	30 s^{-1}
k_{-3}	4.38 s^{-1}	k_7	10^8 M^{-1} s^{-1}

[a] Column entries from k_1 to k_5 are taken from Johnson et al. (*26*) at pH 7.6. Values k_6/k_{-6} and k_7/k_{-7} are from refs 24 and 23, respectively. Equilibrium constants K_1, K_4, K_6, and K_7 were measured as 11.5, 14.9, 0.3, and 1.07 μM, respectively (*23, 24, 26*). A bimolecular rate constant of 10^8 M^{-1} s^{-1} was assumed for k_1, k_{-4}, and k_6 (*26*), allowing the estimation of the dissociation rate constants, k_1, k_{-4}, and k_6. A 10-fold reduction in the association and dissociation rate constants did not significantly influence the outcome of the simulation.

Scheme 1

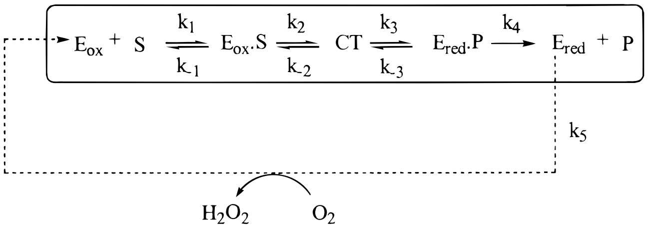

RESULTS AND DISCUSSION

Medium Chain Acyl-CoA Dehydrogenase Studies. Scheme 1 was used by Srivastava and colleagues (*23*) for the oxidase reaction of the MCAD from pig kidney:

The dotted arrows reflect the reoxidation of the 2-electron reduced enzyme by molecular oxygen. The oxidized dehydrogenase (E$_{ox}$) binds indolepropionyl-CoA (S) and the resulting Michaelis−Menten (E$_{ox}$•S) complex advances to a reduced flavin•indoleacryloyl-CoA product charge-transfer complex (CT, formerly designated X; *26*). These reduced flavin•enoyl-CoA charge-transfer complexes are common features of the acyl-CoA dehydrogenases (*2*, *3*, *42*−*44*) and give the medium chain enzyme reduced with octanoyl-CoA a steel-blue color. In the present case, this CT species is reported to decay to a non-charge-transfer reduced enzyme species (E$_{red}$•P; via k_3) followed by the release of product (P, IA-CoA) in step k_4. The reverse reaction (k_{-4}) was ignored (*23*) since P is negligible when initial rates are measured. Reoxidation of the free 2-electron reduced enzyme (E$_{red}$) by molecular oxygen (k_5) completes catalysis of this nonphysiological oxidase reaction of the medium chain enzyme and is depicted by the dotted lines (see legend Scheme 1).

In the first part of this paper, we reconsider Scheme 1 and show that it cannot account for the oxidase activity observed experimentally. All of the values required to model Scheme 1 are taken from the work of Srivastava and colleagues (*23*, *24*, *26*) and are collected and referenced in Table 1. Simulation of the scheme by an iterative routine (see Materials and Methods) gave the IP-CoA dependence at 240 μM oxygen shown in Figure 1 (solid circles). These simulated data are fit to a V_{max} of 0.0082/s and a K_m of 1.58 μM for IP-CoA. These values are in excellent agreement with the steady-state kinetic measurements and the simulations reported by Johnson et al. (*23*; their simulations gave V_{max} 0.008/s, K_m 1.6 μM). The similarity of the observed

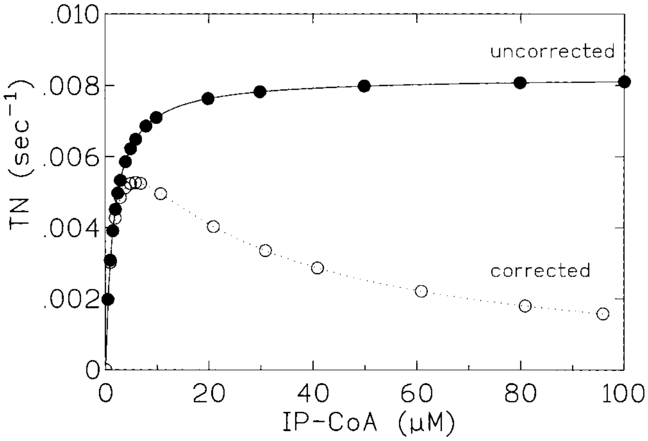

FIGURE 1: Simulated rates for the oxidation of IP-CoA catalyzed by MCAD using molecular oxygen as electron acceptor. Rates were calculated using the data in Table 1 (see Materials and Methods). The solid circles (uncorrected) show the calculated turnover numbers fit to a k_{cat} of 0.0082/s and a K_m of 1.58 μM for IP-CoA. The open circles correct for the binding of IP-CoA to the reduced form of the enzyme (K_d 0.3 μM; *24*, see text).

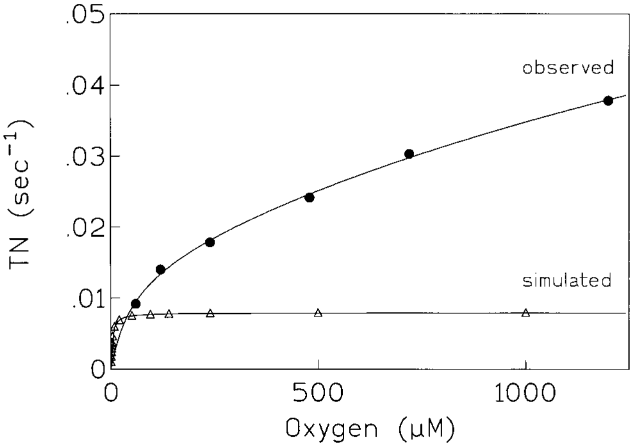

FIGURE 2: Both simulated and experimentally observed dependence of the oxidase activity of pig kidney MCAD on the oxygen concentration using IP-CoA. Steady-state rates were measured (see Materials and Methods) after mixing 30 μM IP-CoA with 2.0 μM pig kidney MCAD in 50 mM phosphate buffer, pH 7.6, 25 °C, using a range of oxygen concentrations. The experimental rates (filled circles) were fit to two processes exhibiting high and low affinities for oxygen with K_m and k_{cat} values of 49 μM and 0.014/s and 3 mM and 0.085/s, respectively). The open triangles show the simulated oxygen dependence obtained from Scheme 1 using 30 μM IP-CoA. Simulated data were fit to a maximal turnover of 0.0079/s and a K_m of 3 μM (see text).

turnover number in the oxidase reaction (0.008/s) with the rate constant for k_3 inferred from an analysis of studies of the reductive half-reaction (0.01/s; *21*) led to the suggestion that this step limited oxygen reactivity (*23*). Thus, the simulated data (labeled uncorrected in Figure 1) match the observed behavior (*23*). The significance of the corrected curve (open circles) will be developed later.

Although the IP-CoA dependence agreed with that predicted by Scheme 1, there was no experimental test of the dependence of the oxidase reaction on the concentration of the second substrate, oxygen (*23*). The triangles in Figure 2 show the simulated oxygen dependence predicted by Scheme 1 using 30 μM IP-CoA. This gives a predicted TN_{max} of 0.0079/s (the IP-CoA concentration of 30 μM is close to saturating) and a K_m for oxygen of 3.0 μM. The apparent affinity for oxygen is high in this simulation because k_3 is so small (0.01/s, Table 1) and rapidly becomes limiting as the oxygen concentration is raised (via $k_5[O_2]$, Scheme 1). The model predicts that oxygen concentrations above 100 μM would be comfortably saturating.

Scheme 2

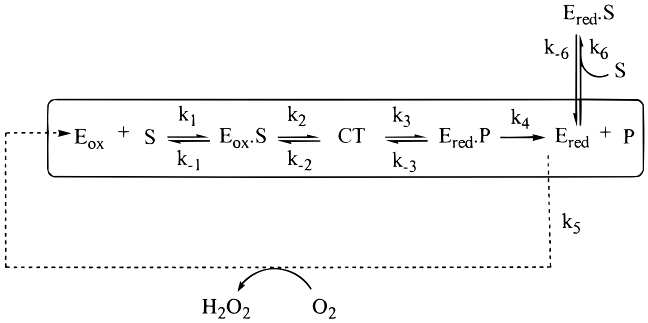

However, our experimentally measured oxygen dependence for the same enzyme under the same conditions (circles, Figure 2) does not resemble the behavior predicted by Scheme 1 and Table 1 (see Materials and Methods). Steady-state rates were measured in the stopped-flow instrument for ease of manipulation of dissolved oxygen concentrations and for a better approximation of initial rates (*45*). A minimum of two kinetic phases is observed experimentally: one saturating at modest oxygen concentrations (K_m, 49 μM; V_{max}, 0.014/s), the other exhibiting an apparent K_m of 3.0 mM (V_{max}, 0.085/s). Clearly, a process with a K_m of 3 μM as predicted by Scheme 1 (Figure 2, triangles) does not make a major contribution to the observed oxidase turnover under these conditions. This pronounced disagreement between predicted and observed behavior prompted additional scrutiny of Scheme 1.

Scheme 1 (*23*) is an oversimplification, because it does not account for complexation of free reduced enzyme (E_{red}) by excess substrate. Such binding of the reduced MCAD to a variety of ligands has been described previously and can be even tighter than to the oxidized enzyme (*12*, *46*, *47*). This is the case for the substrate used here: the K_d values for IP-CoA bound to the reduced and oxidized MCAD are 0.3 and 11.5 μM, respectively (*21*). Inclusion of this additional step (k_6/k_{-6}) yields Scheme 2.

With this additional equilibrium, the concentration of free reduced enzyme would be drastically decreased in favor of E_{red}•S (E_{red}•S/E_{ox} of ca. 100 using 30 μM IP-CoA). If only the free form of the 2-electron reduced enzyme reacts with oxygen, as has been repeatedly suggested (*20*−*28*), then increasing substrate concentration would suppress oxidase activity by sequestering the reduced enzyme as E_{red}•S. The inclusion of this additional step in the simulation yields the open circles in Figure 1 in which the rate would go through a distinct maximum at intermediate IP-CoA concentrations. It is important to note that this predicted excess substrate inhibition above 5 μM IP-CoA (Figure 1) was not encountered experimentally by Srivastava and colleagues: the IP-CoA dependence of the oxidase rate showed Michaelis−Menten kinetics (*20*). We have confirmed these findings, observing no significant substrate inhibition of the oxidase turnover up to 150 μM IP-CoA (data not shown). These results argue strongly that the oxidase activity of the enzyme reduced by IP-CoA cannot be due only to the reaction of the free reduced protein with molecular oxygen (see later). Rather, reoxidation must also involve the reduced enzyme complexed with substrate and some reduced flavin species prior to the rate-limiting step (see later).

We wished to examine which complexes of the reduced dehydrogenase: that with enoyl-CoA product (IA-CoA; as in CT and $E_{red}{\cdot}P$) or that with substrate (IP-CoA; as in $E_{red}{\cdot}S$), were the more reactive toward oxygen. However, a direct assessment with the native reduced enzyme is not feasible. Thus, attempts to generate the reduced enzyme product complexes (CT and $E_{red}{\cdot}P$) by the addition of 1 equiv of substrate to 10 μM oxidized enzyme generates a complex mixture of enzyme species. To simulate this mixture, we used Scheme 2 (including the reverse reaction k_{-4}, Table 1) and set the oxygen concentration at zero. At equilibrium, the enzyme would be distributed as follows: E_{ox} (33.6%), $E_{ox}{\cdot}S$ (6.9%), CT (47.3%), $E_{red}{\cdot}P$ (0.1%), E_{red} (1.4%), and $E_{red}{\cdot}S$ (10.5%). Further, Scheme 2 is itself an oversimplification because it does not include complexation of the oxidized enzyme by any enoyl-CoA product released from reduced enzyme species (Table 1; see later, Scheme 3), a reaction recognized more than 40 years ago (*8*). This introduces yet another species ($E_{ox}{\cdot}P$) comprising 13.5% of the total enzyme with the balance distributed over all the other forms mentioned above (26.2, 5.2, 35.9, 0.1, 2.2, and 16.9%, respectively). Clearly, the preparation of a single species as above is impossible. In addition, the rate of redox equilibration between these enzyme forms is comparable, or faster, than the oxidase reactions to be studied. Hence, the reactivity of the CT and $E_{red}{\cdot}S$ complexes cannot be obtained experimentally with the native enzyme using indolepropionyl-CoA and indoleacryloyl-CoA.

One approach to address this problem is to prevent redox equilibration between enzyme species using the Glu376-Gln mutant of the MCAD. While the mutant enzyme can bind a variety of thioester ligands, it is essentially catalytically inactive because it lacks the base which abstracts the *pro-R*-α-proton from bound substrate (*5*, *48*). The reduced mutant enzyme could then be prepared chemically and subsequently complexed with either IP-CoA or IA-CoA without subsequent redox interconversions. Since the Glu376-Gln mutant is from the human MCAD rather than from the pig kidney source used for our earlier work (*12*), we first compared steady-state turnover values for the wild-type human and pig enzymes with IP-CoA. The human enzyme is some 5-fold less reactive toward oxygen under standard conditions (see Materials and Methods), with a k_{cat} of 0.0028/s in good agreement with that determined earlier (*27*; k_{cat} 0.003/s). The rates of reoxidation of both wild-type and mutant free reduced enzymes in the oxidative half-reaction were then compared using the stopped-flow (see Materials and Methods). Reoxidations at air saturation following the reappearance of the oxidized flavin chromophore at 446 nm were first-order and gave rate constants of 1.35 and 0.83/s for pig and human wild-type enzyme, respectively, at pH 7.6, 25 °C. The rate constant for the pig enzyme compares favorably with the value of 1.03/s determined previously under the same conditions (*23*). The free reduced human Glu376-Gln mutant enzyme is noticeably more reactive toward reoxidation (4.6/s; some 5-fold faster than the wild-type; data not shown). Although it might appear that this increase reflects the elimination of a negative charge near the reduced flavin, the corresponding Glu to Gln mutation in a SCAD has the opposite effect (see later).

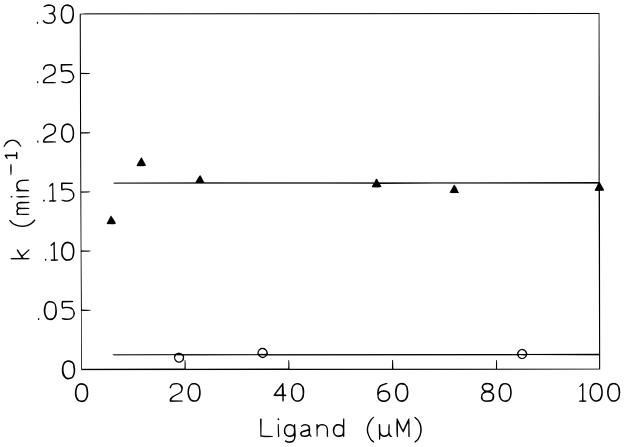

FIGURE 3: Effect of IP- and IA-CoA concentration on the reoxidation of the 2-electron reduced E376Q mutant of MCAD. The mutant in 50 mM potassium phosphate, 0.3 mM EDTA, pH 7.6, was reduced to the dihydroflavin level with sodium dithionite and the IP- or IA-CoA ligands were added with a final oxygen concentration of 240 μM (see Materials and Methods). Rate constants for the first-order return of the oxidized flavin spectrum are plotted as a function of ligand concentration (IP- and IA-CoA, filled triangles and open circles, respectively).

Scheme 3

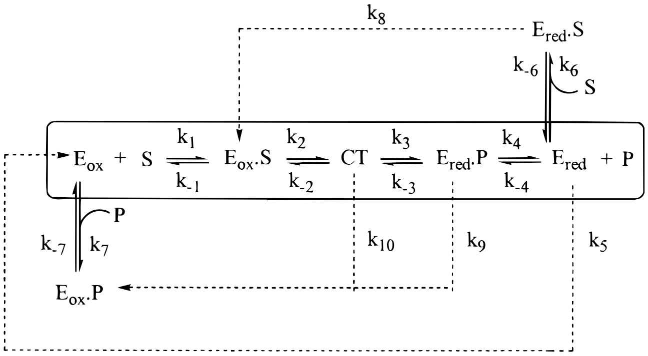

These preliminary experiments with the human MCAD accomplished, Figure 3 shows the effect of increasing IP- and IA-CoA on the reoxidation rate of the free reduced mutant enzyme (see Materials and Methods). Clearly, saturating concentrations of IP-CoA and IA-CoA, while markedly lowering the reactivity of the reduced enzyme toward molecular oxygen, cannot completely suppress reoxidation. Of the two complexes in Figure 3, the substrate (in the $E_{red}{\cdot}S$ species, Scheme 2) is about 10-fold less effective than the charge-transfer complex of the reduced enzyme with IA-CoA. Reoxidation of the charge-transfer complex (*12*) provides a credible explanation of the biphasic response to oxygen concentration seen in Figure 2 (see later). These data are consistent with an oxidase reaction that is much more complicated than previously suggested. Scheme 3 includes all species that might react with oxygen.

Reoxidation of the charge-transfer complex is shown as k_{10}. The other reduced flavin species $E_{red}{\cdot}P$, free E_{red}, and $E_{red}{\cdot}S$ interact with oxygen via k_9, k_5, and k_8, respectively. Since the reoxidation of E_{red} and $E_{red}{\cdot}S$ and, apparently, CT, have been demonstrated in this paper, it is reasonable to assume that the remaining reduced enzyme species $E_{red}{\cdot}P$, deduced by analysis of rapid reaction data (*23*), would also

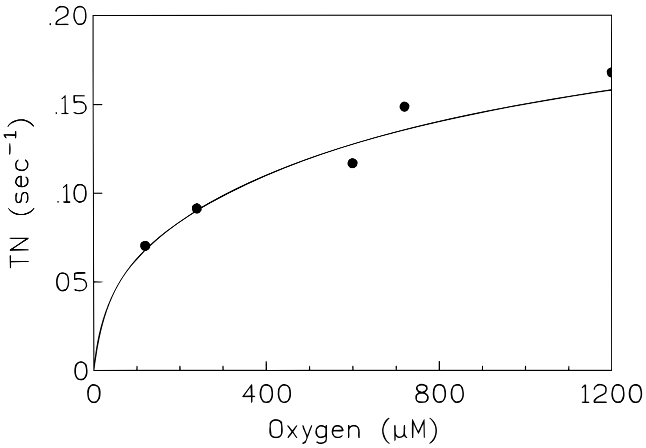

FIGURE 4: Dependence of the oxidase turnover of the pig kidney MCAD using DP-CoA. Turnover was measured as before in the stopped-flow spectrophotometer (see Materials and Methods) to give final concentrations of 2 μM enzyme and 25 μM DP-CoA in 50 mM phosphate buffer, pH 7.6, 25 °C, containing the concentrations of oxygen indicated (see Materials and Methods). The rate of DC-CoA formation was followed at 400 nm (*25*). The experimental rates were fit to two processes exhibiting high and low affinities for oxygen (with K_m and k_{cat} values of 31 μM, 0.057/s and 790 μM, 0.17/s, respectively).

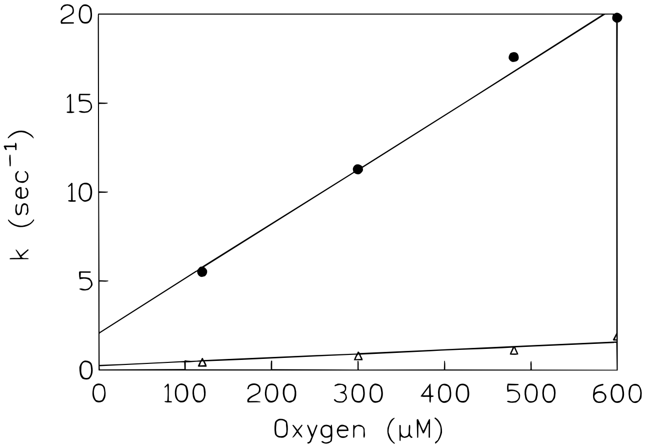

FIGURE 5: Rate constants for the reoxidation of the free dihydroflavin form of SCAD as a function of oxygen concentration. The dehydrogenase was photoreduced as described earlier (*42*) and mixed in the stopped-flow spectrophotometer with 50 mM potassium phosphate buffer, pH 7.0, containing varying amounts of dissolved oxygen (see Materials and Methods). Reoxidation of SCAD was monitored at 450 nm and fit to two exponentials with the slower phase accounting for 15% or less of the total absorbance change. The fast and slow phase rate constants are represented by filled circles and open triangles, respectively.

react with oxygen. Despite the potential complexity of this situation, the biphasic dependence of the steady-state turnover of IP-CoA on oxygen concentration simply requires two points at which oxygen reacts: one before the flux limiting step k_3 (that is k_{10}) and one after it. The fact that three steps are depicted at which oxygen may react after k_3 makes no difference to the simulation; reaction with any one, or any combination, of k_5, k_8, and k_9 will suffice. As the concentration of oxygen is raised from zero, the reoxidation rate $[O_2](k_9[E_{red}{\cdot}P] + k_5[E_{red}] + k_8[E_{red}{\cdot}S])$ begins to make k_3[CT] rate determining since k_3 is so very small. The saturation of this step is responsible for the low K_m for oxygen in the first phase of Figure 2. At higher oxygen concentrations, the reoxidation rate $k_{10}[CT][O_2\ ]$ results in an additional increase in turnover, even after the first phase is saturated. Scheme 3 predicts a limiting rate of 0.55/s given the value of k_2 in Table 1 compared to 0.17/s obtained experimentally.

A second chromophoric substrate of the MCAD, 4-(dimethylamino)-3-phenylpropionyl-CoA, was examined to see whether the biphasic behavior observed above was peculiar to IP-CoA. Oxidation of DP-CoA (*9, 27*) yields the strongly colored cinnamoyl-CoA analogue (DC-CoA; see Materials and Methods; *49*). Steady-state rates were again monitored in the stopped-flow spectrophotometer for ease of manipulation of oxygen concentration and to allow a better approximation of the initial rate. The maximal turnover of 0.11/s at 240 μM oxygen compares favorably with that of Srivastava and co-workers (*25*; 0.088/s) under the same conditions. However, our estimate for the K_m for DP-CoA is some 7-fold lower than theirs (ca. 1.2 μM versus 8.6 μM). Whichever value of the K_m is used, the concentration of substrate employed in Figure 4 (25 μM) is close to saturating. Clearly, a markedly biphasic oxygen dependence of the turnover rate is observed just like that seen with IP-CoA. The solid line in Figure 4 is fit to two Michaelis−Menten processes with values of 0.057/s and a K_m of 31 μM and 0.17/s with a K_m of 790 μM.

These results described show that the biphasic behavior toward molecular oxygen is not peculiar to one particular substrate of the MCAD. Our data with IP-CoA show that the free reduced enzyme is not the only species that reacts with molecular oxygen during oxidase turnover. These studies have been performed with the mammalian MCAD, which shows only modest (<10/min) activity with the best oxidase substrates known and, conversely, extremely slow rates (<0.5/h) with preferred normal substrates such as octanoyl-CoA (*2, 3, 12*).

Bacterial Short Chain Acyl-CoA Dehydrogenase Studies. In an effort to further understand the oxidase reactivity in the acyl-CoA dehydrogenase family, we examined the SCAD from the obligate anaerobe *M. elsdenii* (*50*) because it shows an approximately 5000-fold higher turnover with molecular oxygen when reduced with butyryl-CoA (*3, 53−55*) when compared to substrate-reduced MCAD. The recombinant SCAD (*54*) showed essentially the same maximal oxidase turnover number as that isolated from *M. elsdenii* (32/min vs 30/min but with a somewhat smaller K_m of 5 vs 14 μM; *52*).

Figure 5 shows the oxygen dependence of the rate constants for the reoxidation of the 2-electron reduced SCAD at pH 7.0, 25 °C. Reoxidation at each oxygen concentration shows a major exponential phase of at least 85% of the total with a 15-fold slower phase accounting for the remainder. Both phases are plotted in Figure 5. The rapid phase rate constants (Figure 5, filled circles) can be fit to a straight line with a nonzero intercept in the same manner as those of the MCAD (*23*). This slope of this line yields a bimolecular rate constant for the reoxidation by molecular oxygen of 32 600 $M^{-1}\ s^{-1}$. This value can be compared to that reported for the mammalian MCAD of 2650 $M^{-1}\ s^{-1}$ (*23*). Clearly, this 12-fold difference in the reactivity of the free reduced enzymes does not account for the 5000-fold differences in oxidase activity between short and medium chain dehydrogenases when they are reduced with their optimal substrates (butyryl- and octanoyl-CoA, respectively).

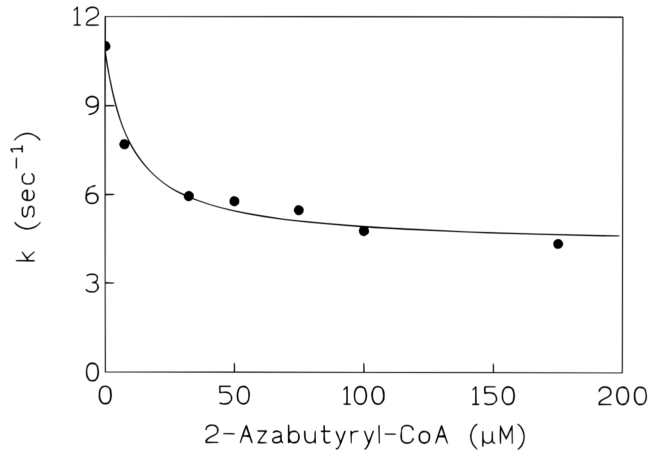

FIGURE 6: Effect of 2-azabutyryl-CoA on the rate constant for the reoxidation of SCAD by oxygen. SCAD was photoreduced anaerobically as described earlier (*42*) and mixed with 2-azabutyryl-CoA to give final concentrations of 4.8 μM protein and 240 μM oxygen in 50 mM KPi, pH 7.0, 0.3 mM EDTA, 25 °C. The resulting data was fit to a K_d value of 6.4 μM with a limiting rate constant of 4.4/s at saturating concentrations of 2-azabutyryl-CoA.

As outlined earlier, saturating concentrations of redox inactive ligands such as 2-azaoctanoyl-CoA exert a profound slowing (ca. 3000-fold) of the reoxidation of the MCAD by molecular oxygen. Figure 6 shows a comparable experiment with SCAD in the presence of increasing concentrations of 2-azabutyryl-CoA. In sharp contrast to the mammalian case, saturating levels of 2-azabutyryl-CoA effect less than a 3-fold slowing of oxygen reactivity. Prior spectroscopic and electrochemical studies showed that 2-azabutyryl-CoA was an excellent ligand of the bacterial enzyme (*47*). However, the failure to substantially protect against reoxidation with molecular oxygen might conceivably reflect some unanticipated peculiarity of the thioester analogue. Hence, we utilized the Glu367-Gln mutant of the short chain dehydrogenase to allow the rate of reoxidation of complexes of the reduced enzyme with both the true substrate and product (butyryl- and crotonyl-CoA) to be assessed. As before, elimination of the catalytic base yields an inactive enzyme (*54*) and permits full formation of complexes of the reduced enzyme with saturating levels of substrate or product without the complication of additional redox steps. Figure 7 (open triangles) shows that butyryl-CoA exerts essentially no protection on the reduced enzyme up to 200 μM. As expected, the corresponding product, crotonyl-CoA, forms a charge-transfer complex with the reduced mutant enzyme (λ_{max}, 566 nm; data not shown) but still only offers about 5-fold protection (filled circles, Figure 7). The corresponding protection of the medium chain dehydrogenase by *trans*-2-octenoyl-CoA is greater than 5000-fold.

CONCLUSIONS

This work shows that the oxidase reaction of the MCAD toward IP-CoA does not simply reflect reoxidation of the free enzyme as has been suggested recently (*20−28*), but includes contributions from additional reduced enzyme species. Amending Scheme 1 to include equilibria known to participate in the reductive half of catalysis (see above) requires that both E_{red}·S and CT react with oxygen. If E_{red}·S was unreactive, then the oxidase turnover would show significant product inhibition (see earlier). If CT failed to react in Scheme 3, the second phase responsible for the increased reactivity at higher oxygen concentrations would not be seen. Studies with the Glu376-Gln mutant of the human MCAD clearly show that both ligated species retain appreciable reactivity. It is important to note that these experiments with a human mutant enzyme cannot provide kinetic data for detailed modeling of the observed reactivity of the pig kidney enzyme. First, while the properties of pig and human enzymes are generally very similar (*27, 48, 55, 56*), the human enzyme is conspicuously less reactive toward oxygen in overall turnover using IP-CoA (*22*). Second, kinetic constants that can only be obtained for an inactive Glu376-Gln mutant cannot be assumed to apply to the wild-type enzyme, especially because this particular carboxylate appears to modulate oxygen reactivity in unpredictable ways (see above).

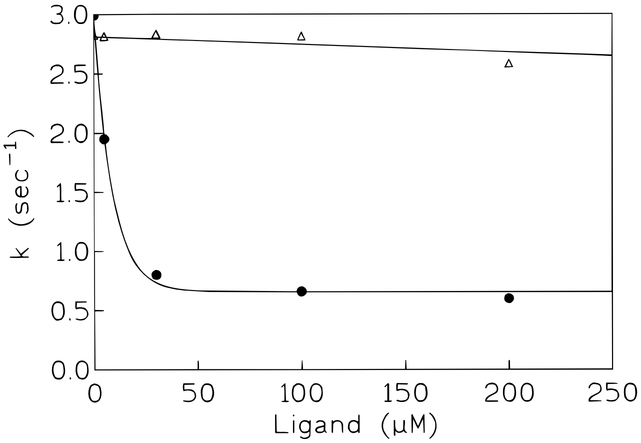

FIGURE 7: Effect of butyryl- and crotonyl-CoA on the reoxidation of the 2-electron reduced form of the E367Q mutant of SCAD. The reduced mutant enzyme was prepared by dithionite titration and mixed in the stopped-flow spectrophotometer with solutions of butyryl- or crotonyl-CoA in phosphate buffer, pH 7.0, containing 480 μM dissolved oxygen. The first-order return of the oxidized flavin spectrum at 450 nm is plotted as a function of ligand concentration (open triangles, butyryl-CoA; filled circles, crotonyl-CoA).

The studies in which redox equilibration is avoided using the Glu376-Gln mutant extend earlier work in which redox-inactive thioester analogues were used with the native medium chain enzyme. In these prior experiments, saturating concentrations of some ligands, particularly those lacking the thioester carbonyl group, were almost ineffective, whereas a variety of thioesters such as 3-thia- and 2-aza-octanoyl-CoA exerted approximately 3000-fold protection (*12*). These data are clear: saturating concentrations of ligands do not necessarily completely suppress oxygen reactivity in the medium chain enzyme.

An observation cited in ref 26 to support the suggestion that only the free dihydroflavin form of acyl-CoA dehydrogenase reacts directly with oxygen was the behavior of lactate oxidase (monooxygenase) from *Mycobacterium smegmatis*. Massey and co-workers clearly demonstrated that the pyruvate complex of the semiquinone form of this enzyme reacts very slowly with oxygen at a rate limited by the dissociation of ligand (*57*). However, their studies also showed that, in the case of the dihydroflavin form of the oxidase (and it is the dihydroflavin form of acyl-CoA dehydrogenase which is the principal concern here), the situation is just the reverse: now reoxidation by molecular oxygen is much faster than dissociation. Further, recent mutagenesis experiments with lactate oxidase show how small changes in the active site can profoundly affect the course of oxidative turnover of lactate (*58−60*). More generally, there are a number of examples in which a flavoprotein oxidase shows either ping-pong or ternary complex mechanisms, depending on the nature of the first substrate. Thus, selection of a single literature example to support a claim that only the free form of the MCAD reacts with oxygen is unwarranted.

This work shows that ligation can only weakly suppress the oxygen reactivity of the short chain enzyme (by up to about 5-fold for the reduced enzyme•crotonyl-CoA complex, see earlier). Why, then, is the corresponding protection for the *trans*-2-octenoyl-CoA complex of the reduced MCAD dramatically greater? Presumably, the mammalian enzyme is under significant evolutionary pressure to minimize the metabolically wasteful and potentially deleterious reduction of dioxygen. In contrast, the obligate anaerobe *M. elsdenii*, does not encounter oxygen under normal metabolic conditions and has not evolved to suppress its intrinsic oxidase activity (*6, 12, 61*). The crystal structure of the bacterial dehydrogenase shows that the active site remains more solvent accessible than that of the mammalian enzyme upon complexation (*6, 35, 55, 56, 62*). There are both theoretical and experimental reasons to propose that solvation plays a significant role in modulation of the reactivity of reduced flavins toward molecular oxygen (*6, 12*). With the mammalian enzyme, the thorough desolvation of key regions of the active site by good ligands may therefore contribute to low oxidase activity. In contrast, oversized thioesters such as IP− CoA (with V_{max}/K_m values some 500-fold smaller than those of octanoyl-CoA; *20*) appear relatively poorly accommodated and may desolvate the active site less efficiently. It will be interesting to determine high-resolution crystal structures of complexes of the MCAD with a range of oxidase substrates to see whether a correlation between structure and activity emerges.

ACKNOWLEDGMENT

We thank Dr. Mahendra Jain for helpful discussions, Drs. Arnold Strauss and Sandro Ghisla for gifts of wild-type and Glu376-Gln human MCAD *E. coli* strains, and Dr. Grant Mauk for running preliminary stopped-flow experiments on SCAD.

REFERENCES

1. Massey, V. (1994) *J. Biol. Chem. 269*, 22459−22462.
2. Beinert, H. (1963) in *The Enzymes* (Boyer, P. D., Lardy, H., and Myrback, K., Eds.) 2nd ed. Vol. 7, pp 447−466, Academic Press, New York.
3. Engel, P. C. (1992) in *Chemistry and Biochemistry of Flavoenzymes* (Muller, F., Ed.) Vol. III, pp 597−655, CRC Press, Boca Raton, FL.
4. Tanaka, K., and Indo, Y. (1992) in *New Developments in Fatty Acid Oxidation*, pp 95−110, Wiley-Liss, Inc., New York.
5. Ghisla, S., Engst, S., Vock, P., Kieweg, V., Bross, P., Nandy, A., Rasched, I., and Strauss, A. W. (1994) in *Flavins and Flavoproteins* (Yagi, K., Ed.) pp 283−292, Walter de Gruyter, Berlin.
6. Thorpe, C., and Kim, J.-J. P. (1995) *FASEB J. 9*, 718−725.
7. Crane, F. L., and Beinert, H. (1956) *J. Biol. Chem. 218*, 717−731.
8. Beinert, H., and Page, E. (1957) *J. Biol. Chem. 225*, 479−497.
9. Murfin, W. W. (1974) Ph.D. Thesis, Washington University, St. Louis, MO.
10. Hall, C. L., Lambeth, J. D., and Kamin, H. (1979) *J. Biol. Chem. 254*, 2023−2031.
11. Thorpe, C., Matthews, R. G., and Williams, C. H. (1979) *Biochemistry 18*, 331−337.
12. Wang, R., and Thorpe, C. (1991) *Biochemistry 31*, 7895−7901.
13. Cummings, J. G., Lau, S.-M., Powell, P. J., and Thorpe, C. (1992) *Biochemistry 31*, 8523−8529.
14. Reinsch, J., Katz, A., Wean, J., Aprahamian, G., and McFarland, J. T. (1980) *J. Biol. Chem. 255*, 9093−9097.
15. Gorelick, R. J., Schopfer, L. M., Ballou, D. P., Massey, V., and Thorpe, C. (1985) *Biochemistry 24*, 6830−6839.
16. Gorelick, R. J., and Thorpe, C. (1986) *Biochemistry 25*, 7092−7098.
17. Thorpe, C. (1991) in *Chemistry and Biochemistry of Flavoenzymes* (Muller, F., Ed.) Vol. II, pp 471−486, CRC Press, Boca Raton, FL.
18. Lenn, N. D., Stankovich, M. T., and Liu, H.-w. (1990) *Biochemistry 29*, 3709−3715.
19. Muller, F., Jarbandhan, T., Gast, R., and Grande, H. J. (1975) in Reactivity of Flavins (Yagi, K., Ed.) pp 51−70, University of Tokyo Press, Tokyo.
20. Johnson, J. K., Wang, Z.-X., and Srivastava, D. K. (1992) *Biochemistry 31*, 10564−10575.
21. Johnson, J. K., and Srivastava, D. K. (1993) *Biochemistry 32*, 8004−8013.
22. Johnson, J. K., Kumar, N. R., and Srivastava, D. K. (1993) *Biochemistry 32*, 11575−11585.
23. Johnson, J. K., Kumar, R. N., and Srivastava, D. K. (1994) *Biochemistry 33*, 4738−4744.
24. Kumar, N. R., and Srivastava, D. K. (1994) *Biochemistry 33*, 8833−8841.
25. Srivastava, D. K., Kumar, N. R., and Peterson, K. L. (1995) *Biochemistry 34*, 4625−4632.
26. Kumar, N. R., and Srivastava, D. K. (1995) *Biochemistry 34*, 9434−9443.
27. Peterson, K. L., Sergienko, E. E., Wu, Y., Kumar, N. R., Strauss, A. W., Oleson, A. E., Muhonen, W. W., Shabb, J. B., and Srivastava, D. K. (1995) *Biochemistry 34*, 14942−14953.
28. Srivastava, D. K., Wang, S., and Peterson, K. L. (1997) *Biochemistry 36*, 6359−6366.
29. McFarland, J. T., Lee, M.-Y., Reinsch, J., and Raven, W. (1982) *Biochemistry 21*, 1224−1229.
30. Bernert, J. T., and Sprecher, H. (1977) *J. Biol. Chem. 252*, 6736−6744.
31. Boudjouk, P., and Han, B. H. (1983) *J. Catal. 79*, 489−492.
32. Cummings, J. G., and Thorpe, C. (1994) *Biochemistry 33*, 788−797.
33. Bedzyk, L. A., Escudero, K. W., Gill, R. E., Griffin, K. J., and Frerman, F. E. (1993) *J. Biol. Chem. 268*, 20211−20217.
34. Lau, S.-M., Powell, P., Buettner, H., Ghisla, S., and Thorpe, C. (1986) *Biochemistry 25*, 4184−4189.
35. Nandy, A., Kieweg, V., Krautle, F.-G., Vock, P., Kuchler, B., Bross, P., Kim, J.-J. P., Rasched, I., and Ghisla, S. (1996) *Biochemistry 35*, 12402−12411.
36. Becker, D. F., Fuchs, J. A., and Stankovich, M. T. (1994) *Biochemistry 33*, 7082−7087.
37. Williamson, G., and Engel, P. C. (1984) *Biochem. J. 218*, 521−529.
38. Lehman, T. C., Hale, D. E., Bhala, A., and Thorpe, C. (1990) *Anal. Biochem. 186*, 280−284.
39. Engel, P. C. (1981) *Methods Enzymol. 71*, 359−366.
40. Massey, V., and Hemmerich, P. (1978) *Biochemistry 17*, 9−17.
41. Lehman, T. C., and Thorpe, C. (1990) *Biochemistry 29*, 10594−10602.
42. Massey, V., and Ghisla, S. (1974) *Ann. N. Y. Acad. Sci. 22*, 446−465.
43. Thorpe, C., and Massey, V. (1983) *Biochemistry 22*, 2972−2978.
44. Lau, S.-M., and Thorpe, C. (1988) *Arch. Biochem. Biophys. 262*, 293−297.

45. Entsch, B., Ballou, D. P., Husain, M., and Massey, V. (1976) *J. Biol. Chem. 251*, 7376−7379.
46. Schopfer, L. M., Massey, V., Ghisla, S., and Thorpe, C. (1988) *Biochemistry 27*, 6599−6611.
47. Pace, C. P., and Stankovich, M. T. (1994) *Arch. Biochem. Biophys. 313*, 261−266.
48. Bross, P., Engst, S., Strauss, A. W., Kelly, D. P., Rasched, I., and Ghisla, S. (1990) *J. Biol. Chem. 265*, 7116−7119.
49. D'Ordine, R. L., Tonge, P. J., Carey, P. R., and Anderson, V. E. (1994) *Biochemistry 33*, 12635−12643.
50. Engel, P. C., and Massey, V. (1971) *Biochem. J. 125*, 879−887.
51. Engel, P. C., Williamson, G., and Shaw, L. (1984) in *Flavins and Flavoproteins* (Bray, R. C., Engel, P. C., and Mayhew, S. G., Eds.) pp 403−412, Walter de Gruyter, Berlin.
52. Ellison, P., Shaw, L., Williamson, G., and Engel, P. C. (1984) in *Flavins and Flavoproteins* (Bray, R. C., Engel, P. C., and Mayhew, S. G., Eds.) pp 413−416, Walter de Gruyter, Berlin.
53. Ellison, P., and Engel, P. C. (1987) in *Flavins and Flavoproteins* (Edmondson, D. E., and McCormick, D. B., Eds.) pp 181−183, Walter de Gruyter, Berlin.
54. Becker, D. F., Fuchs, J. A., Banfield, D. K., Funk, W. D., MacGillivray, T. A., and Stankovich, M. T. (1993) *Biochemistry 32*, 10736−10742.
55. Kim, J.-J. P., Wang, M., and Paschke, R. (1993) *Proc. Natl. Acad. Sci. U.S.A. 90*, 7523−7527.
56. Lee, H.-J. K., Wang, M., Paschke, R., Nandy, A., Ghisla, S., and Kim, J.-J. P. (1996) *Biochemistry 35*, 12412−12420.
57. Choong, Y. S., and Massey, V. (1980) *J. Biol. Chem. 255*, 8672−8677.
58. Muh, U., Massey, V., and Williams, C. H., Jr. (1994) *J. Biol. Chem. 269*, 7982−7988.
59. Muh, U., Massey, V., and Williams, C. H., Jr. (1994) *J. Biol. Chem. 269*, 7989−7993.
60. Muh, U., Massey, V., and Williams, C. H., Jr. (1994) *J. Biol. Chem. 269*, 7994−8000.
61. Engel, P. C. (1990) in *Chemistry and Biochemistry of Flavoenzymes* (Muller, F., Ed.) Vol. III, pp 597−655, CRC Press, Boca Raton, FL.
62. Djordjevic, S., Pace, C. P., Stankovich, M. T., and Kim, J.-J. P. (1995) *Biochemistry 34*, 2163-2171.

BI980767S